Portugaliae Electrochimica Acta 26 (2008) 211-220

PORTUGALIAE ELECTROCHIMICA ACTA

Pyrazole Derivatives as Corrosion Inhibitors for Steel in Hydrochloric Acid

L. Herrag, A. Chetouani, S. Elkadiri, B. Hammouti,* A. Aouniti

*Laboratoire de Chimie Appliquée & Environnement, Faculté d*es Sciences,
Université Mohammed 1st, 60000 Oujda, Morocco

Received 17 May 2007; accepted 9 August 2007

Abstract

The effect of 1-{[benzyl-(2-cyano-ethyl)-amino]-methyl}-5-methyl-1H-pyrazole-3-carboxylic acid methyl ester (P1) and 1-{[benzyl-(2-cyano-ethyl)-amino]-methyl}-5-methyl-1H-pyrazole-3-carboxylic acid ethyl ester (P2) was evaluated as corrosion inhibitors of steel in molar hydrochloric using weight loss measurements and electrochemical polarisation. The results obtained reveal that those compounds reduce the corrosion rate. The inhibiting action increases with the concentration of pyrazole compounds to attain 98.5 % at the 10^{-3} M of (P2). The increase in temperature leads to a decrease in the inhibition efficiency of the compounds in the temperature range 308 – 353 K. The adsorption isotherm of inhibitors on the steel has been determined. The thermodynamic data of activation and adsorption are determined.

***Keywords**:* pyrazole, inhibition, corrosion, steel, acid.

Introduction

Hydrochloric acid is commonly used in industrial processes like chemical cleaning and pickling to remove mill scales (oxide scales) from the metal surface. During this stage, the addition of inhibitor is necessary to avoid the attack of metal. Inhibitors should be effective even under severe conditions in concentrated acid (20%) and temperatures ranging from 60 to 95 °C. The most efficient corrosion inhibitors used in chlorhydric acid contain heteroatoms such as sulphur, nitrogen and oxygen containing compounds [1-6].

* Corresponding author. E-mail address: hammoutib@yahoo.fr

Survey of literature reveals that azole, azine and pyridine [7-9] compounds are effective corrosion inhibitors up to 80 °C. The synthesis of new organic molecules offers various molecular structures containing several heteroatoms and substituants. Their adsorption is generally explained by the formation of an adsorptive film of a physical or chemical character on the metal surface [10-12]. The encouraging results obtained by pyrazolic compounds [13-17] have incited us to synthesize other compounds and to test their addition on the corrosion behaviour of steel in acidic media.

In the present work, we investigate the corrosion of steel in 1 M HCl by 1-{[benzyl-(2-cyano-ethyl)-amino]-methyl}-5-methyl-1H-pyrazole-3-carboxylic acid methyl ester (P1) and 1-{[benzyl-(2-cyano-ethyl)-amino]-methyl}-5-methyl-1H-pyrazole-3-carboxylic acid ethyl ester (P2); weight loss and polarisation measurements have been used to study the effect of addition of these compounds on the corrosion of steel in HCl solution. The effect of temperature is also studied and some thermodynamic parameters are evaluated.

Experimental details

Steel sample containing 0.09%P; 0.38%Si; 0.01%Al; 0.05%Mn; 0.21%C; 0.05%S and the remainder iron. Prior to all measurements, the steel samples are polished with different emery paper up to 1200 grade, washed thoroughly with bidistilled water degreased and dried with ethanol, acetone.

The molar hydrochloric solution is prepared by dilution of Analytical Grad 97% HCl with bidistilled- water.

Pyrazole compounds were synthesised by aza-type *Michael* addition [18-19], purified and characterised by N.M.R and mass spectroscopy before use. The molecular structure of the pyrazole studied is shown in Fig. 1.

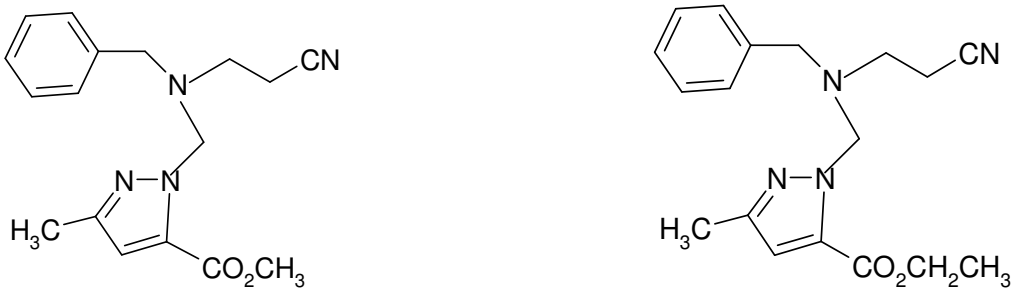

P1 **P2**

Figure 1. Molecular structure of 1-{[benzyl-(2-cyano-ethyl)-amino]-methyl}-5-methyl-1H-pyrazole-3-carboxylic acid methyl ester (P1) and 1-{[benzyl-(2-cyano-ethyl)-amino]-methyl}-5-methyl-1H-pyrazole-3-carboxylic acid ethyl ester (P2).

Gravimetric measurements are carried out in double walled glass cell equipped with a thermostatic cooling condenser. The solution volume is 100 cm^3. The steel specimens used have a rectangular form (1.5 cm × 1.5 cm × 0.05 cm).

Electrochemical trends are carried out in a conventional three electrode cylindrical glass cell. The working electrode, in the form of a disc cut from steel, has a geometric area of 1 cm^2. A saturated calomel electrode (SCE) and platinum electrode are used as reference and auxiliary electrode, respectively. The temperature is thermostatically controlled at 308 K. The polarisation curves are recorded with a potentiostat type EG and G 273, at a scan rate of 30 mV/min. The steel electrode was maintained at corrosion potential for 30 min and thereafter pre-polarised at − 800 mV for 10 min. The potential was swept to anodic potentials. The test solution is de-aerated for 30 min in the cell with pure nitrogen which is maintained throughout the experiments.

Results and discussion

Weight loss measurements

Table 1 resumes the corrosion rate obtained in 1 M HCl (W^0_{corr}) and at various contents of P1 and P2 (W_{corr}) determined at 308 K after 1 h of immersion rate and inhibition efficiencies E_w, determined by the relation:

$$E_w\% = 100 \times \left(1 - \frac{W_{Corr}}{W^\circ_{Corr}}\right) \quad (1)$$

where W_{corr} and $W°_{corr}$ are the corrosion rates of steel with and without P1 and P2, respectively.

Table 1. Gravimetric results of steel in 1 M HCl with and without addition of the compounds P1 and P2 at various concentrations.

Inhibitor	Concentration (M)	W ($mg.cm^{-2}.h^{-1}$)	E %
	Blanc	1.439	-
P1	10^{-6}	1.284	10.7
	10^{-5}	0.991	31.0
	5×10^{-5}	0.147	89.7
	10^{-4}	0.13	90.9
	5×10^{-4}	0.114	92.1
	10^{-3}	0.033	97.7
P2	10^{-6}	0.71	50.7
	10^{-5}	0.387	73.1
	5×10^{-5}	0.207	85.6
	10^{-4}	0.105	92.7
	5×10^{-4}	0.0738	94.9
	10^{-3}	0.0218	98.5

It is clear that the addition of compounds reduces the corrosion rate in HCl solution. The inhibitory effect increases with the increase of pyrazoles derivatives concentration. E% reaches a maximum of 98% at 10^{-3} M for P2. The effectiveness of P2 is due to the presence of ethyl group which has more inductive effect compared to methyl one in P1. The protective properties of these

compounds are probably due to the interaction between π-electrons of the pyrazole rings and heteroatom with positively charged steel surface [20-21]. We may conclude that compounds are good inhibitors of steel corrosion in 1 M HCl solution.

Electrochemical polarisation measurements

In the case of polarisation method the relation determines the inhibition efficiency (*E%*):

$$E\% = 100 \times \left(1 - \frac{I_{Corr}}{I^{\circ}_{Corr}}\right) \quad (2)$$

where I°_{corr} and I_{corr} are the uninhibited and inhibited corrosion current densities, respectively, determined by extrapolation of cathodic Tafel lines to corrosion potential.

Polarisation behaviour of steel in 1 M HCl in the presence and absence of inhibitors is shown in Fig. 2. The values of corrosion current (I_{corr}), corrosion potential (E_{corr}), cathodic Tafel slope (b_c) and inhibition efficiency (E%), are collected in Table 2.

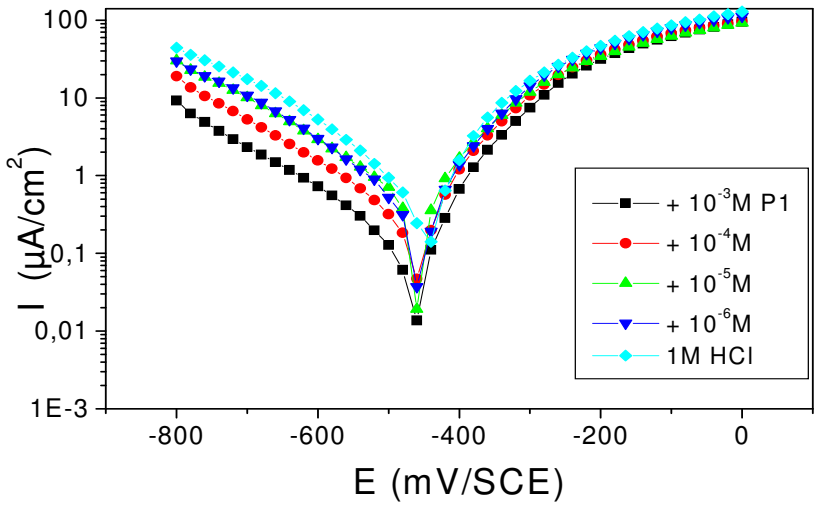

Figure 2. Typical polarisation curves of steel in 1 M HCl for various concentrations of P1.

The examination of Fig. 2 and Table 2 shows that the addition of P1 and P2 decreases current density. The decrease is more pronounced with the increase of the inhibitor concentration. The Tafel plots indicate that the mechanism of hydrogen reduction is activation control. The presence of pyrazoles does not affect the cathodic Tafel slope, indicating that the mechanism of H^+ reduction is not modified with the P1 and P2 concentration. Also, the corrosion potential is almost constant in the presence of the inhibitors. But in the anodic domain, the i–E characteristics are almost the same. This result indicates that organic compounds act predominantly as cathodic inhibitors by simple blocking the

available surface area. The inhibitor molecules decrease the surface area of corrosion and only cause inactivation of a part of the surface with respect to the corrosion medium. The inhibition efficiency reaches 90.6 and 91.5 % at 10^{-3} M of P1 and P2, respectively. This phenomenon is interpreted by the adsorption of the molecules on steel surface leading to the increase of the surface coverage θ defined by E% / 100. E% increases with compound concentration. We may conclude that P1 and P2 are effective inhibitors of steel corrosion in molar HCl.

Table 2. Polarisation parameters for steel in acid at different contents of P1 and P2 at 308 K.

Concentration	E_{corr} (mV)	b_c (mV/ dec)	I_{corr} (μA/cm^2)	E%
1 M HCl	-475	178	1239.6	-
10^{-6} M P1	-516	170	1141.6	7.9
10^{-5} M P1	-511	179	916.4	26.1
10^{-4} M P1	-454	172	234.5	81.1
10^{-3} M P1	-467	165	116.4	90.6
10^{-6} M P2	-480	180	638	48.5
10^{-5} M P2	-461	173	397	68.0
10^{-4} M P2	-438	184	177	85.7
10^{-3} M P2	-454	162	106	91.5

Effect of temperature

We have studied the temperature influence on the efficiency of P1 an P2. For this purpose, we made weight-loss measurements in the temperature range 313-353 K, in the presence and absence of the compound at various concentrations during 1 h of immersion. The corresponding data are shown in Table 3.

It is clear that the increase of corrosion rate is more pronounced with the rise of temperature for blank solution. In the presence of the tested molecules, W_{corr} is highly reduced. Hence we note that the efficiency depends on the temperature and dercreases with the rise of temperature from 308 to 353 K. This can be explained by the decrease of the strength of the adsorption process at elevated temperature and suggested a physical adsorption mode.

To calculate activation thermodynamic parameters of the corrosion reaction such as the energy Ea, the entropy ΔS° and the enthalpy ΔH° of activation, Arrhenius Eq. (2) and its alternative formulation called transition state Eq. (3) were used:

$$W = K \exp\left(-\frac{E_a}{RT}\right) \tag{3}$$

$$W = \frac{RT}{Nh}\exp\left(\frac{\Delta S_a^o}{R}\right)\exp\left(-\frac{\Delta H_a^o}{RT}\right) \tag{4}$$

where T is the absolute temperature, K is a constant and R is the universal gas constant, h is Plank's constant, and N is Avogadro's number.

Table 3. Effect of temperature on the corrosion rate of steel at various concentrations of P2 at 1 h.

Temperature (K)	Concentration (M)	W ($mg/cm^2.h$)	E (%)	θ
313	Blanc	2.604	-	-
	5×10^{-5}	0.905	65.2	0.652
	10^{-4}	0.460	82.3	0.823
	5×10^{-4}	0.242	90.7	0.907
	10^{-3}	0.201	92.3	0.923
323	Blanc	4.834	-	-
	5×10^{-5}	1.877	61.2	0.612
	10^{-4}	0.965	80.1	0.801
	5×10^{-4}	0.574	88.2	0.882
	10^{-3}	0.482	90.0	0.900
333	Blanc	8.7815	-	-
	5×10^{-5}	3.998	54.5	0.545
	10^{-4}	2.824	67.8	0.678
	5×10^{-4}	1.598	81.8	0.818
	10^{-3}	0.969	89.0	0.890
343	Blanc	13.235	-	-
	5×10^{-5}	9.372	29.2	0.292
	10^{-4}	7.971	39.8	0.398
	5×10^{-4}	4.927	62.8	0.628
	10^{-3}	3.562	73.1	0.731
353	Blanc	26.552	-	-
	5×10^{-5}	21.176	20.2	0.202
	10^{-4}	20.049	24.5	0.245
	5×10^{-4}	11.205	57.8	0.578
	10^{-3}	9.588	63.9	0.639

The activation energy E_a is calculated from the slope of the plots of $\ln(W_{corr})$ vs. 1 / T (Fig. 3). Plots of $\ln(W_{corr} / T)$ vs. 1 / T give a straight line with a slope of $\Delta H° / R$ and an intercept of $(\mathrm{Log}(R / Nh) + \Delta S° / R)$, as shown in Fig. 4. From this relation the values of $\Delta H°$ and $\Delta S°$ can be calculated (Table 4).

The decrease of P1 and P2 efficiencies with temperature rise leads to a higher value of E_a, when compared to that in an uninhibited acid, and it is interpreted as an indication of an electrostatic character of the inhibitor's adsorption [22]. But, Ea variation is not the unique parameter to affirm of such mode of adsorption. Other ones can be considered, such as free adsorption enthalpy ΔG^0_{ads} and enthalpy ΔH^0_{ads}, which will be discussed in next paragraph. The positive values of $\Delta H°$ mean that the dissolution reaction is an exothermic process and that the dissolution of steel is difficult [23]. Practically E_a and $\Delta H°$ are of the same order. Also, the entropy $\Delta S°$ increases more positively with the presence of the inhibitor

than in the presence of the non-inhibited one. This reflects the formation of an ordered stable layer of the inhibitor on the steel surface [24]. From the previous data, we can conclude that P2 is an effective inhibitor.

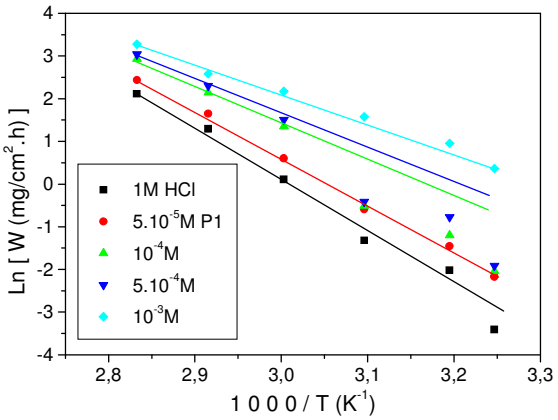

Figure 3. Typical Arrhenius plots for log W vs. 1 / T for steel in 1 M HCl at different concentrations of P1.

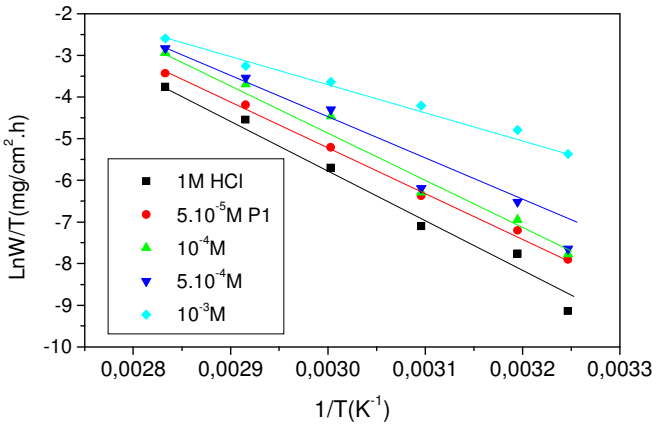

Figure 4. The relation between log (*W* / *T*) vs. 1 / *T* for steel at different concentrations of P1.

Table 4. Activation parameters of the dissolution of steel in 1 M HCl in the absence and presence of P1 and P2.

C (M)	E_a (kJ/mol)	ΔH°_a (kJ/mol)	ΔS°_a (J/mol.K)	E_a-ΔH°_a (kJ/mol)
Blank	55.27	52.5	-70.6	2.7
5×10^{-5} P1	99.18	96.4	53.3	2.7
10^{-4} P1	101.83	99.1	59.8	2.7
5×10^{-4} P1	92.95	90.2	29.7	2.7
10^{-3} P1	107.33	104.6	68.4	2.7
5×10^{-5} P2	84.59	81.8	11.4	2.7
10^{-4} P2	98.55	95.8	50.4	2.7
5×10^{-4} P2	96.90	94.2	41.0	2.7
10^{-3} P2	93.15	90.4	27.7	2.7

Adsorption isotherm

Fig. 5 shows the linear dependence of θ / 1 – θ as a function of concentration C of the inhibitors, where θ is the surface coverage determined by the ratio *E%* / 100. Inhibitor adsorbs on the steel surface according to the Langmuir kind isotherm model which obeys the relation:

$$(5)\ \frac{\theta}{1-\theta} = KC$$

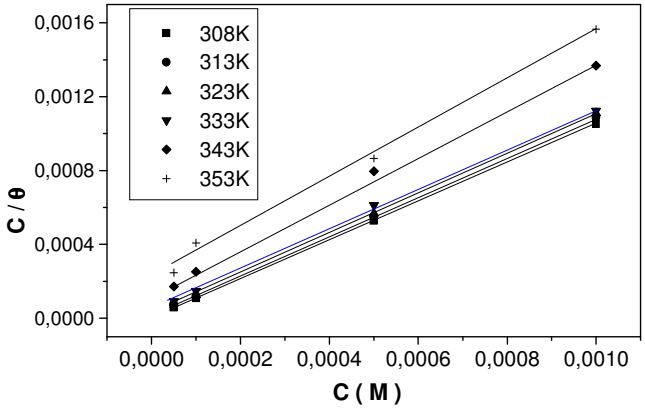

Figure 5. Fitting Langmuir's adsorption isotherm model for P2 in 1 M HCl at different temperatures.

The thermodynamic parameters for adsorption given in Table 5 were calculated using the values of K according to the following relations:

$$\ln(K) = -\frac{\Delta H^{\circ}_{ads}}{\mathrm{R\,T}} + Constant \qquad (6)$$

$$K = \frac{1}{55.5}\exp(-\frac{\Delta G^{\circ}}{\mathrm{RT}}) \qquad (7)$$

$$\frac{\Delta G^{\circ}_{ads}}{T} = \frac{\Delta H^{\circ}_{ads}}{T} + A \qquad (8)$$

$$\Delta G^{\circ}_{ads} = \Delta H^{\circ}_{ads} - T\Delta S^{\circ}_{ads} \qquad (9)$$

where ΔS^{0}_{ads} and ΔH^{0}_{ads} are the entropy and the enthalpy of activation, respectively. From this relation the values of ΔH^{0}_{ads}, ΔS^{0}_{ads} and ΔG^{0}_{ads} can be calculated (Table 5).

The negative values of ΔG°_{ads} suggest that the adsorption of P2 molecule onto the steel surface is a spontaneous process and the adsorbed layer is stable. Generally values of ΔG°_{ads} around -20 kJ/mol or lower are consistent with the electrostatic interaction between the charged molecules and the charged metal (physisorption), those around -40 kJ/mol or higher involve charge transfer from organic molecules to the metal at the surface to form a coordinate type of bond (chemisorption) [25-27]. The calculated ΔG°_{ads} close – 40 kJ/mol indicates that

chemisorption is a probable process. But, values of other thermodynamic parameter as ΔH_{ads} can provide supplementary information about the mechanism

Table 5. Thermodynamic data for studied P2 from experimental adsorption isotherm.

Temperature (K)	*K*	$\Delta G°_{ads}$ (kJ mol^{-1})	$\Delta H°_{ads}$ (kJ mol^{-1})	$\Delta S°_{ads}$ (J $.mol^{-1}K^{-1}$)
308	230360.1	-41.93		
313	51724.2	-38.72		
323	45284.5	-39.60	-70.85	-97.4
333	22793.7	-38.92		
343	7853.0	-37.06		

of corrosion inhibition. While an endothermic adsorption process ($\Delta H_{ads} > 0$) is attributed unequivocally to chemisorption, an exothermic adsorption process ($\Delta H_{ads} < 0$) may involve either physisorption or chemisorption or a mixture of both processes [28, 29]. In the present work, the negative value obtained may introduce a mixture of both chemisorption and physisorption processes. This may be interpreted by the presence of both heteroatoms (four nitrogen and two oxygen atoms) which lead to coordinate bonds and aromatic rings which get physisorption. Also the negative values of $\Delta H°_{ads}$ show that the adsorption is exothermal with an ordered phenomenon ascribed by the negative values of $\Delta S°_{ads}$. This order may more probably be explained by the possibility of formation of iron complex on the metal surface [30, 31].

Conclusions

From the overall experimental results the following conclusions can be deduced:

- The 1-{[benzyl-(2-cyano-ethyl)-amino]-methyl}-5-methyl-1H-pyrazole-3-carboxylic acid methyl ester (P1) and 1-{[benzyl-(2-cyano-ethyl)-amino]-methyl}-5-methyl-1H-pyrazole-3-carboxylic acid ethyl ester (P2) are efficient inhibitors for the corrosion of steel in 1 M HCl.
- The inhibition efficiency of P2 increases with the concentration to attain a maximum value 98.5% at 10^{-3} M.
- P1 and P2 act as cathodic inhibitors with modifying the hydrogen reduction mechanism.
- The inhibition efficiency of P1 and P2 decreases with the rise of temperature.
- The activation and adsorption thermodynamic parameters are determined.

References

1. G. Mengoly, M.M. Musiani, C. Pagura, F. Paoulucci, *Corros. Sci.* 31 (1991) 743.
2. D. Bouzidi, S. Kertit, B. Hammouti, M. Brighli, *J. Electrochem. Soc. India* 46 (1997) 23.
3. S. Kertit, K. Bekkouch, B. Hammouti, *Revue de Métallurgie (Paris)* 97 (1998) 251.

4. Y. Abed, B. Hammouti, F. Touhami, A. Aouniti, S. Kertit, A. Mansri, K. Elkacemi, *Bull. Electrochem*. 17 (2001) 105.
5. F.B. Growcock, V.R. Lopp, *Corros. Sci*. 28 (1998) 397.
6. G. Quartarone, T. Bellomi, A. Zingales, *Corros. Sci*. 45 (2003) 715.
7. M. Bouklah, A. Attayibat, B. Hammouti, A. Ramdani, S. Radi, M. Benkaddour, *Appl. Surf. Sci*. 240 (2005) 341.
8. A. Aouniti, B. Hammouti, S. Kertit, *Bull. Electrochem*. 14 (1998) 193.
9. K.M. El-Sobki, H. Abbas, *React. Solids* 5 (1988) 191.
10. G. Subramaniam, K. Balasubramanian, P. Sridhar, *Corros. Sci.* 30 (1990) 1019.
11. Y. Xiao-Ci, Z. Hong, L. Ming-Dao, R. Hong-Xuan, Y. Lu-An, *Corros. Sci*. 42 (2000) 645.
12. M. Lashkari, M.R. Arshadi, *Chem. Phys*. 299 (2004) 131.
13. M. Benabdellah, R. Touzani, A. Aouniti, A. Dafali, S. El Kadiri, B. Hammouti, M. Benkaddour, *Mater. Chem. Phys*. (2007). In press.
14. K. Tebbji, I. Bouabdellah, A. Aouniti, B. Hammouti, H. Oudda, M. Benkaddour and A. Ramdani, *Materials Letters* 61 (2007) 799.
15. A. Chetouani, M. Daoudi, B. Hammouti, T. Ben Hadda and M. Benkaddour, *Corros. Sci.* 48 (2006) 2987.
16. K. Tebbji, B. Hammouti, H. Oudda, A. Ramdani and M. Benkadour, *Appl. Surf. Sci*. 252 (2005) 1378.
17. M. Elayyachy, M. Elkodadi, A. Aouniti, A. Ramdani, B. Hammouti, F. Malek, A. Elidrissi, *Mater. Chem. Phys*. 93 (2005) 281.
18. L. Herrag, R. Touzani, A. Ramdani, B. Hammouti, *Molbank* 2006, M493
19. L. Herrag, R. Touzani, A. Ramdani, B. Hammouti, *Molbank* 2006, M494
20. A. Chetouani, B. Hammouti, A. Aouniti, N. Benchat, T. Benhadda, *Prog. Org. Coat*. 45 (2002) 373.
21. A. Chetouani, A. Aouniti, B. Hammouti, N. Benchat, T. Benhadda, S. Kertit, *Corros. Sci*. 45 (2003) 1675.
22. A. Popova, *Corros. Sci*. 49 (2007) 2144.
23. N.M. Guan, L. Xueming, L. Fei, *Mater. Chem. Phys*. 86 (2004) 59.
24. A. Yurt, A. Balaban, S.U. Kandemir, G. Bereket, B. Erk, *Mater. Chem. Phys*. 85 (2004) 420.
25. M. Bouklah, N. Benchat, B. Hammouti, A. Aouniti, S. Kertit, *Materials Letters* 60 (2006) 1901.
26. F.M. Donahue, K. Nobe, *J. Electrochem. Soc*. 112 (1965) 886.
27. E. Khamis, F. Bellucci, R.M. Latanision, E.S.H. El-Ashry, *Corrosion* 47 (1991) 677.
28. W. Durnie, R.D. Marco, A. Jefferson, B. Kinsella, *J. Electrochem. Soc*. 146 (1999) 1751.
29. S.A. Ali, A.M. El-Shareef, R.F. Al-Ghamdi, M.T. Saeed, *Corros. Sci*. 47 (2005) 2659.
30. M. Abdallah and M. M. El-Naggar, *Mater. Chem. Physics* 71 (2001) 291.
31. A. Bousseksou, G. Molnár, J.A. Real, K. Tanaka, *Coord. Chem. Rev*. 251 (2007) 1822.